Supporting Information: Market Optimization and Technoeconomic Analysis of Hydrogen-Electricity Coproduction Systems

Daniel J. Laky[1,†], Nicole P. Cortes[1,†], John C. Eslick[2], Alexander Noring[2], Naresh Susarla[2], Chinedu Okoli[2], Miguel A. Zamarripa-Perez[2], Douglas Allan[2], John H. Brewer[3], Arun K.S. Iyengar[2], Maojian Wang[2], Anthony P. Burgard[4], David C. Miller[4], Alexander Dowling[1] corresponding email - adowling@nd.edu

[1] *Department of Chemical and Biomolecular Engineering*
University of Notre Dame, Notre Dame, IN 46556, USA
[2] *National Energy Technology Laboratory site support contractor*
Pittsburgh, PA 15236, USA
[3] *National Energy Technology Laboratory*
Morgantown, WV 15236, USA
[4] *National Energy Technology Laboratory*
Pittsburgh, PA 15236, USA

S1. PROMOD ERCOT Region Simulations

To generate the simulations for these scenarios, the generating resource list in the existing ERCOT simulation-ready dataset for Hitachi Energy's PROMOD IV was modified using the May 2021 Power Forecast Capacity Expansion from IHSMarkit using the processes and procedures detailed by Brewer and Labarbara [76], particularly those described in Section 3.2 of the procedures covering Uncertain Additions, with modification to adjust the starting point to match that detailed for 2031 in the December 2021 ERCOT Capacity, Demand, and Reserves Report [77]. Since the IHS forecast does not include unit-specific details and required capacity reductions in specific generating types, a capacity retirement schedule was developed that retired unit capacity pro rata based on a combination of age and period escalated operating costs. While PROMOD utilizes a monthly basis differential model for natural gas pricing, given the proximity to Henry Hub and concentration of natural gas-fired resources near major Texas load centers, the net effect resulted in an average annualized system-wide natural gas-fired generation fuel price of \$4.30$\cdot$MMcf^{-1} (\$4.42$\cdot$MMBtu^{-1}). Additionally, the energy and peak demand projections from the IHS forecast were disaggregated to the four load zones represented in PROMOD IV using weighted percentages based on recent non-pandemic year operating data.

Upon implementation and execution, following these processes, initial production cost runs indicated a 450 MW system imbalance resulting in expected unserved energy in the Houston transmission zone. In order to resolve this, both a transmission and generation solution were examined. In the transmission solution, the Houston-South bi-directional interface was increased by 500 MW. This interface was selected for modification over the Houston-North interface because it is currently smaller and has equal flow limits (4,880 MW forward/reverse), while the Houston-North interface is rated predominantly for flow into the Houston zone (1,960 MW forward / 6,582 MW reverse). For the generation solution, a single NGCC deployment added through the uncertain addition process was shifted to the Houston zone from the North zone, resolving the Houston zone expected unserved energy, while also leaving sufficient generating capacity in the North zone. Upon testing, the generation solution resulted in lower system prices; those prices were chosen for evaluation in this paper.

S2. Market-Optimization Formulation

The following formulation details the MINLP used to solve for optimal annual profit. Table S1 defines all symbols used in the mathematical formulation:

$$\max_{\substack{\bar{f}^{\text{profit}}, f^{\text{profit}}, \\ y,v,w,p,h}} \quad \sum_{m\in\mathcal{B}}\sum_{t\in\mathcal{T}} \bar{f}^{\text{profit}}_{m,t} - \sum_{t\in\mathcal{T}} \left(\theta^u v_t + \theta^d w_t\right) \tag{S1a}$$

$$\begin{aligned}
\text{s.t.} \quad f^{\text{profit}}_{m,t} &= \pi^e_t p_{m,t} + \pi^h h_{m,t} \\
&\quad - \frac{\pi^g}{\bar{\pi}^g} f^{\text{fuel}}_m(p_{m,t}, h_{m,t}) \\
&\quad - f^{\text{var}}_m(p_{m,t}, h_{m,t}) \\
&\quad - \pi^c f^{\text{carbon}}_m(p_{m,t}, h_{m,t}) && \forall m\in\mathcal{B}, \forall t\in\mathcal{T} \quad \text{(S1b)} \\
&\quad - f^{\text{fixed}}(P^{\max}, H^{\max}) \\
&\quad - \frac{\pi^e_t}{\bar{\pi}^e} f^{\text{elec}}_m(h_{m,t}) \\
\bar{f}^{\text{profit}}_{m,t} &\le f^{\text{profit}}_{m,t} - M^l_{m,t}(1 - y_{m,t}), && \forall m\in\mathcal{B}, \forall t\in\mathcal{T} \quad \text{(S1c)}
\end{aligned}$$

$$\bar{f}^{\text{profit}}_{m,t} \leq M^u_{m,t} y_{m,t}, \qquad \forall m \in \mathcal{B}, \forall t \in \mathcal{T} \tag{S1d}$$

$$\sum_{m \in \mathcal{A}} y_{m,t} = 1, \qquad \forall t \in \mathcal{T} \tag{S1e}$$

$$y_{\text{on},t} = 1 - y_{\text{off},t}, \qquad \forall t \in \mathcal{T} \tag{S1f}$$

$$v_t \geq y_{\text{on},t} - y_{\text{on},t-1}, \qquad \forall t \in \mathcal{T} \tag{S1g}$$

$$w_t \geq y_{\text{on},t-1} - y_{\text{on},t}, \qquad \forall t \in \mathcal{T} \tag{S1h}$$

$$\sum_{j=t-\tau^u+1}^{t} v_j \leq y_{\text{on},t}, \qquad \{t \in \mathcal{T} : t > \tau^u\} \tag{S1i}$$

$$\sum_{j=t-\tau^d+1}^{t} w_j \leq 1 - y_{\text{on},t}, \qquad \{t \in \mathcal{T} : t > \tau^d\} \tag{S1j}$$

$$(p_{m,t}, h_{m,t}) \in \mathcal{G}_m, \qquad \forall m \in \mathcal{A}, \forall t \in \mathcal{T} \tag{S1k}$$

Table S1: Mathematical symbols used in the optimization formulation

Symbol	Definition
Sets	
$\mathcal{A}$	Set of all operating modes
$\mathcal{B}$	Set of operating modes excluding "off"
$\mathcal{T}$	Set of all time points
$\mathcal{G}_m$	Feasible region of power and H_2 production for mode m
Parameters	
$P^{\max}$	Maximum power output of the system in MW
$H^{\max}$	Maximum H_2 output of the system in kg·s^{-1}
$M^u_{m,t}$	Upper big-M for mode m at time t in \$·hr^{-1}
$M^l_{m,t}$	Lower big-M for mode m at time t in \$·hr^{-1}
θ^u	Start-up cost in \$
θ^d	Shut-down cost in \$

Symbol	Definition
τ^d	Minimum down time in hr
τ^u	Minimum up time in hr
π^c	Carbon tax in \$$\cdot$tonne^{-1}
π_t^e	LMP at time t in \$$\cdot$MWh^{-1}
$\bar{\pi}^e$	Reference LMP in \$$\cdot$MWh^{-1}
π_t^g	Natural gas price at time t in \$$\cdot$MMBtu^{-1}
$\bar{\pi}^g$	Reference natural gas price in \$$\cdot$MMBtu^{-1}
π^h	H_2 selling price in \$$\cdot$kg^{-1}
Variables	
$h_{m,t}$	H_2 generation for mode m at time t in kg$\cdot$hr^{-1}
$p_{m,t}$	Power generation for mode m at time t in MW
v_t	Binary, 1 if system starts up at time t, 0 otherwise
w_t	Binary, 1 if system shuts down at time t, 0 otherwise
$y_{m,t}$	Binary, 1 if mode m is active at time t, 0 otherwise
$y_{\text{on},t}$	Binary, 1 if any mode $m \in \mathcal{B}$ is active at time t, 0 otherwise
Functions	
$f_m^{\text{carbon}}(p_{m,t}, h_{m,t})$	Carbon output in tonne$\cdot$hr^{-1}
$f_m^{\text{elec}}(h_{m,t})$	Electricity cost in \$$\cdot$hr^{-1}
$f^{\text{fixed}}(P^{\max}, H^{\max})$	Fixed cost in \$$\cdot$hr^{-1}
$f_m^{\text{fuel}}(p_{m,t}, h_{m,t})$	Fuel cost in \$$\cdot$hr^{-1}
$f_m^{\text{var}}(p_{m,t}, h_{m,t})$	Variable cost in \$$\cdot$hr^{-1}
$f_{m,t}^{\text{profit}}$	Profit in \$$\cdot$hr^{-1} for mode m at time t
$\bar{f}_{m,t}^{\text{profit}}$	Relaxed profit in \$$\cdot$hr^{-1} for mode m at time t

The problem is indexed over two sets: $t \in \mathcal{T}$, all time points in the simulation horizon, and $m \in \mathcal{A}$, a set of all possible operating modes. The set $\mathcal{A}$ changes based on what operating modes are available for a specific technology (see Figure 1). The objective (equation S1a) is to maximize profit. The first term, $\bar{f}^{\text{profit}}_{m,t}$, represents the relaxed profit of each mode m at each timestep t. The second term represents start-up costs, θ^u, and shut-down costs, θ^d, at each timestep, which are only accrued at timestep t when binary variables v_t and w_t are active (or have a value of 1), respectively.

The big-M constraints in equations S1c and S1d imply two things: (1) when mode m is active, the relaxed profit, $\bar{f}^{\text{profit}}$, for that mode is less than or equal to the profit, $f^{\text{profit}}_{m,t}$, and less than or equal to $M^u_{m,t}$, and (2) when mode m is not active, the relaxed profit must be less than or equal to zero and less than or equal to $f^{\text{profit}}_{m,t} - M^l_{m,t}$ (which will always be less than zero). Since profit is maximized in the objective function, the profit will always be at the upper bound, so with these constraints, the relaxed profit, $\bar{f}^{\text{profit}}$, will either be equivalent to the profit, f^{profit}, when mode m is active and zero when mode m is not active.

Equation S1b describes the net revenue of the system, f^{profit}. The first two terms represent revenue from power and H_2 sales, respectively. Then, all the cost equations are subtracted from the revenue including fuel cost, variable cost, carbon tax, fixed cost, and electricity cost (only included for models that produce H_2 using grid electricity). f^{carbon}_m is calculated by the fuel usage of the system. Assuming full conversion of the natural gas, and taking the carbon capture percentage into account, the carbon emissions can be calculated. Fuel usage surrogates are reported in Eslick et al. (2023) [49]. Surrogates that were fit with a reference selling price (f^{fuel}_m and f^{elec}_m) are corrected for the actual natural gas price and LMP using the actual value divided by the reference value. Since the fixed costs of a given system are the same for all modes, the fixed cost term is removed during numerical solution of the optimization problem.

$M^l_{m,t}$ must be at most the minimum profit for a mode with a given LMP, and $M^u_{m,t}$ must be at least the maximum profit for a mode at a given LMP. Since it is time-consuming to run the max/min profit optimization for every LMP, we run a range of LMPs and interpolate to get the max/min profit estimate for each time point. To calculate $M^l_{m,t}$, we subtract 20% from the minimum profit, and to calculate $M^u_{m,t}$, we add 20% to the maximum profit.

Equation S1e allows only one mode to be active at a time, and equation S1f gathers when any equipment is "on."

Equation S1g states that the startup variable, v_t, is one if the system went from being off at time $t-1$ to on at time t, and zero otherwise. Similarly, S1h states that shutdown variable, w_t, is one if the system went from being on at time $t-1$ to off at time t, and zero otherwise. Since there is a cost associated with startup and shutdown (equation S1a), startup and shutdown of the system will only take place if the action results in higher profit margins. Equations S1i and S1j enforce the minimum up time, τ^u, and minimum down time, τ^d, constraints (more information available in [78]). Also, see SI Table S2 for start-up/shut-down costs and minimum up and down times.

In addition to the listed equations, constraints enforcing a ramping rate for each system were included in the original formulation. However, all systems can ramp from the minimum to maximum output in significantly less than an hour, so they were ultimately excluded when optimizing these systems. Ramping rates are also included in SI Table S2. This assumption is consistent with other analyses on solid oxide-based systems [46].

Table S2: Ramping, Start-Up, and Shut-Down data for each System Concept

	NGCC	SOFC	NGCC + SOEC		rSOC		SOFC + SOEC		SOEC
	power	*power*	*power*	H_2	*power*	H_2	*power*	H_2	H_2
Start-Up Time	0.1 hrs	24 hrs	24 hrs		24 hrs		24 hrs		24 hrs
Shut-Down Time	0.9 hrs	36 hrs	36 hrs		36 hrs		36 hrs		36 hrs
Start-Up Cost	\$2,898	\$162,015	\$181,404		\$162,015		\$285,146		\$162,015
Shut-Down Cost	\$176	\$89,330	\$98,457		\$89,330		\$157,221		\$89,330
Ramping Rates	70 $\frac{\text{MW}}{\text{min}}$	100 $\frac{\text{MW}}{\text{min}}$	70 $\frac{\text{MW}}{\text{min}}$	1 $\frac{\text{kg/s}}{min}$	100 $\frac{\text{MW}}{\text{min}}$	1 $\frac{\text{kg/s}}{min}$	100 $\frac{\text{MW}}{\text{min}}$	1 $\frac{\text{kg/s}}{min}$	1 $\frac{\text{kg/s}}{min}$
Minimum Up/Down Time	0.07 hrs/0.04 hrs	24 hrs/36 hrs	24 hrs/36 hrs		24 hrs/36 hrs		24 hrs/36 hrs		24 hrs/36 hrs

S3. Market Optimization Solution Procedure

The market optimization problem was solved using a two-step procedure. First, the problem was solved using Dicopt but formulated with bilinear terms where the profit in the objective for each mode is multiplied by the binary variable that represents whether the mode is active and the big-M constraints are omitted. Dicopt will solve this problem using a non-linear programming relaxation, and the result is feasible but not necessarily optimal. The initialization problem solves quickly and reliably. The result of the bilinear problem is used to initialize the problem as formulated with big-M constraints in Section S2 to obtain the optimal solution. For both the initialization and final problem, the default Dicopt settings were used.

Table S3 lists each process concept's minimum, average, and maximum computation times in minutes. The problems were solved on an Apple M1 processor with 8 GB of RAM.

Table S3: Minimum, average, and maximum computational time across all cases for each system

Process Concept	**Minimum Time (min)**	**Average Time (min)**	**Maximum Time (min)**
NGCC	0.32	0.78	2.14
SOFC	0.55	1.47	4.15
NGCC + SOEC	2.17	8.96	123.59
rSOC	0.82	3.61	22.95
SOFC + SOEC	2.65	12.42	97.88
SOEC	0.23	1.49	17.59

S4. LMP Statistics

Multimodal distributions have more than one local maxima rather than one [79]. We utilize two different statistical metrics to determine whether our selected signals are multimodal or unimodal. The first is the bimodality coefficient, which is defined by an empirical relationship between multimodality and third-order (skewness - m_3) and fourth-order (kurtosis - m_4) statistics [80, 81]. The formula for the coefficient, BC, is as follows [82]:

$$BC = \frac{m_3^2 + 1}{m_4 + \frac{3(n-1)^2}{(n-2)(n-3)}} \tag{S1}$$

Here, when $BC \geq 0.555$, a distribution can be considered bimodal or multimodal, with a value of 1.0 obtained for a Bernoulli distribution. Values $BC < 0.555$ can be considered unimodal or heavy-tailed of any modality [82].

We also use Hartigan's dip test to rule out unimodality. Here, the dip test statistic is defined as the maximum difference between the empirical distribution function and the unimodal distribution function that minimizes that maximum difference [83]. The dip test statistic and p-value determine if this difference is great enough to reject the null hypothesis (unimodality). The dip test statistic measures deviation from unimodality, with a smaller value indicating the distribution is close to unimodal and a larger value indicating the distribution is far from unimodal. Literature suggests that both statistics have strengths, but neither is specific or sensitive enough to reliably predict multimodality [84]. In Figure 3, we identify 13 electricity price scenarios with a bimodality coefficient greater than 0.555 and dip test statistic greater than 0.05 as biomodal or multimodal.

S5. Linear Regression

We performed multivariate linear regression on optimal annual profit results using economic conditions as features. We regress the coefficients of the following equation:

$$\mathbf{y} = \beta^T \mathbf{X} \tag{S1}$$

For a set of m dependent variables and n features, $\mathbf{X}$ is an $n \times m$ matrix of features, β is a $1 \times n$ vector of coefficients to be fit, and $\mathbf{y}$ is an $m \times 1$ vector of dependent variables. Here, our dependent variables are the optimal profits for each case, and the features are natural gas price (in \$$\cdot$MMBtu^{-1}); H_2 price (in \$$\cdot$kg^{-1}); mean LMP; minimum LMP; 25$^{\text{th}}$, 50$^{\text{th}}$ and 75$^{\text{th}}$ percentile LMP; maximum LMP, standard deviation (in \$$\cdot$MWh^{-1}); skewness of the LMP signal; kurtosis of the LMP signal; the bimodality coefficient; and the dip test statistic. We started by standardizing all features across the scenarios using the following equation:

$$x_i \leftarrow \frac{x_i - \mu_{x_i}}{\sigma_{x_i}} \tag{S2}$$

where x_i represents the unstandardized feature, μ_{x_i} represents the mean value of that feature across all the market scenarios, and σ_{x_i} represents the standard deviation of the feature across all market scenarios. The case annual profits are also standardized across all cases using the following equation:

$$\mathbf{y} \leftarrow \frac{\mathbf{y} - \mu_y}{\sigma_y} \tag{S3}$$

where $\mathbf{y}$ is the case optimal profit, μ_y is the mean annual profit value across every process concept and market scenario, and σ_y is the standard deviation across every process concept and market scenario. See SI Table S4 for all means and standard deviations used to standardize features and profit values. After standardizing, we use an ordinary least squares objective to fit β values for each of the above features. We used the `statsmodels` version 0.13.5 linear regression function to conduct the regression and obtain the coefficients, intercepts, and R^2 values in Table S5 (see Section 4.5).

Table S4: Means and Standard Deviations of Linear Regression Features

Feature	**Mean**	**Standard Deviation**
Natural Gas Price ($/MMBtu)	4.09	2.25
Carbon Tax ($/tonne)	35.33	56.02
Hydrogen Price ($/kg)	2.00	0.71
Mean LMP ($/MWh)	42.69	19.48
Minimum LMP ($/MWh)	-56.40	101.09
25th Percentile ($/MWh)	24.09	16.20
Median LMP ($/MWh)	35.81	21.57
75th Percentile ($/MWh)	54.46	27.00
Maximum LMP ($/MWh)	1546.74	1549.95
Standard Deviation ($/MWh)	56.05	36.85
Skewness	10.71	10.95

Feature	**Mean**	**Standard Deviation**
Kurtosis	335.88	354.64
Bimodality Coefficient	0.62	0.23
Dip Test Statistic	0.03	0.04
Optimal Profit (M$)	29.98	76.69

Table S5: Linear regression coefficients for each technology type. All features were standardized before regression was performed. Annual profits were standardized across technologies. Bold font and * denote coefficients that are statistically significant ($p<0.05$).

	NGCC	**SOFC**	**NGCC + SOEC**	**rSOC**	**SOFC + SOEC**	**SOEC**
Natural Gas Price ($/MMBtu)	**-0.18***	**-0.26***	**-0.62***	**-0.27***	**-0.52***	-0.05
Carbon Tax ($/tonne)	**0.34***	**0.21***	**0.28***	**0.45***	**0.28***	**0.18***
Hydrogen Price ($/kg)	0	0	**0.59***	**0.51***	**0.63***	**0.64***
Mean LMP ($/MWh)	**0.89***	**0.89***	**1.05***	**1.06***	**1.01***	0
Minimum LMP ($/MWh)	-0.01	0	-0.03	-0.03	-0.02	-0.03
25^{th} Percentile ($/MWh)	**-0.28***	**-0.14***	**-0.35***	**-0.55***	**-0.34***	**-0.27***
Median LMP ($/MWh)	0.01	0.01	-0.13	-0.11	-0.09	-0.10
75^{th} Percentile ($/MWh)	**-0.28***	**-0.16***	-0.37	**-0.41***	-0.30	-0.21
Maximum LMP ($/MWh)	**-0.18***	**-0.17***	-0.17	**-0.38***	**-0.31***	-0.19
Standard Deviation (MWh)	**0.18***	**0.16***	0.17	**0.38***	**0.31***	**0.2***
Skewness	**0.05***	**0.05***	-0.03	-0.02	-0.02	-0.06
Kurtosis	**0.03***	**0.03***	0.09	**0.15***	**0.12***	**0.10***
Bimodality Coefficient	**-0.05***	**-0.05***	-0.06	**-0.10***	-0.08	-0.05
Dip Test Statistic	0.04	**0.04***	-0.09	**-0.10***	-0.10	-0.13
Intercept	**-0.9***	**-0.16***	**-0.57***	**0.69***	**0.72***	**0.22***
R^2	0.98	0.99	0.88	0.88	0.92	0.90

S6. Linear Regression: Correlation Matrix Analysis

Figure S1 shows the correlations between the linear regression features. The strongest feature correlation, 0.87, is between the LMP signal's maximum value and standard deviation. As expected, there are also strong positive correlations between the mean and percentile statistics for LMP: 0.85 between mean LMP and median LMP, 0.81 between mean and 75^{th} percentile, and 0.71 between mean and 25^{th} percentile. Moreover, mean LMP and natural gas price have a positive correlation of 0.64, which is expected because a significant fraction of the generators in each market relies on natural gas. The standard deviation of the signal is moderately correlated with the bimodality coefficient (0.59) and moderately negatively correlated with the dip test statistic (-0.22). This is expected as all three metrics point to considerable variation in the signal. The dip test statistic is also negatively correlated with natural gas price (-0.57) and 25^{th} percentile LMP (-0.4), indicating a market with higher gas prices and LMPs may be more likely to be unimodal. Conversely, this suggests that lower natural gas prices result in more volatile electricity pricing, possibly due to other less flexible resources being dispatched first, such as coal. Carbon tax is positively correlated with the dip test statistic (0.69), indicating signals with carbon taxes are less likely to be unimodal. This also may be due to the LMP scenarios we utilized to project the effect of carbon taxes, many of which included high renewables penetration.

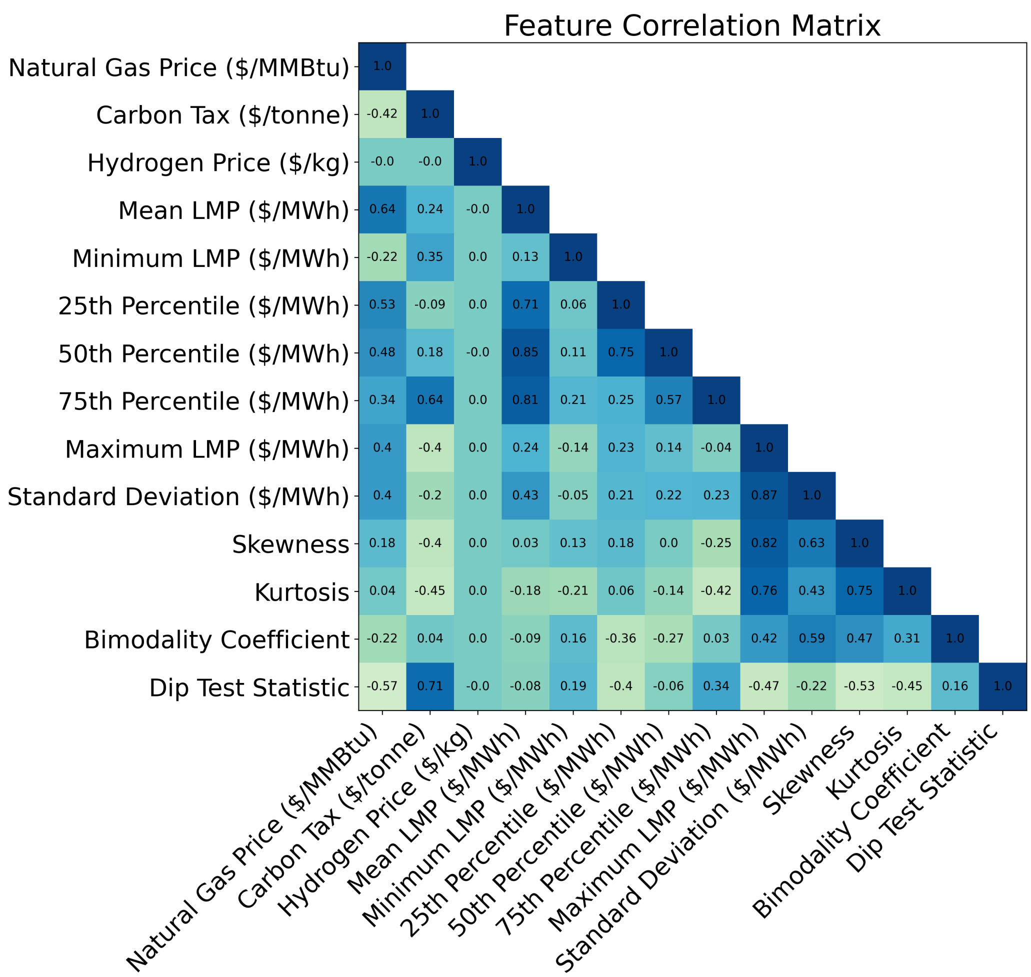

Figure S1: Correlation between features for linear regression

S7. Marginal Cost Plots and Break Even Analysis

The following section of SI is a series of plots for the marginal cost of power, H_2, or a combination of both in those systems that can produce power and H_2. Also, break even plots for the systems at natural gas prices of \$4.42·MMBtu^{-1} and \$8.00·MMBtu^{-1} are presented for each technology.

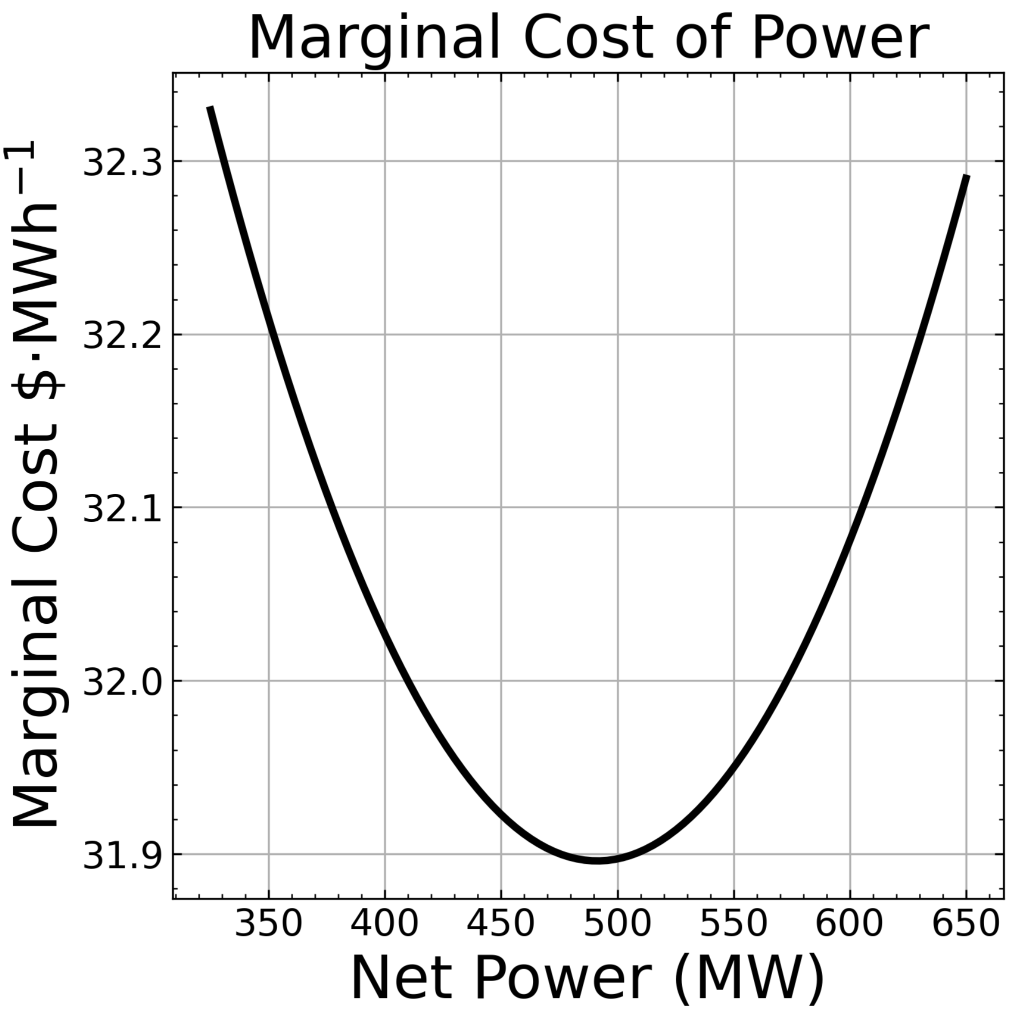

Figure S2: Marginal cost of power for standalone NGCC.

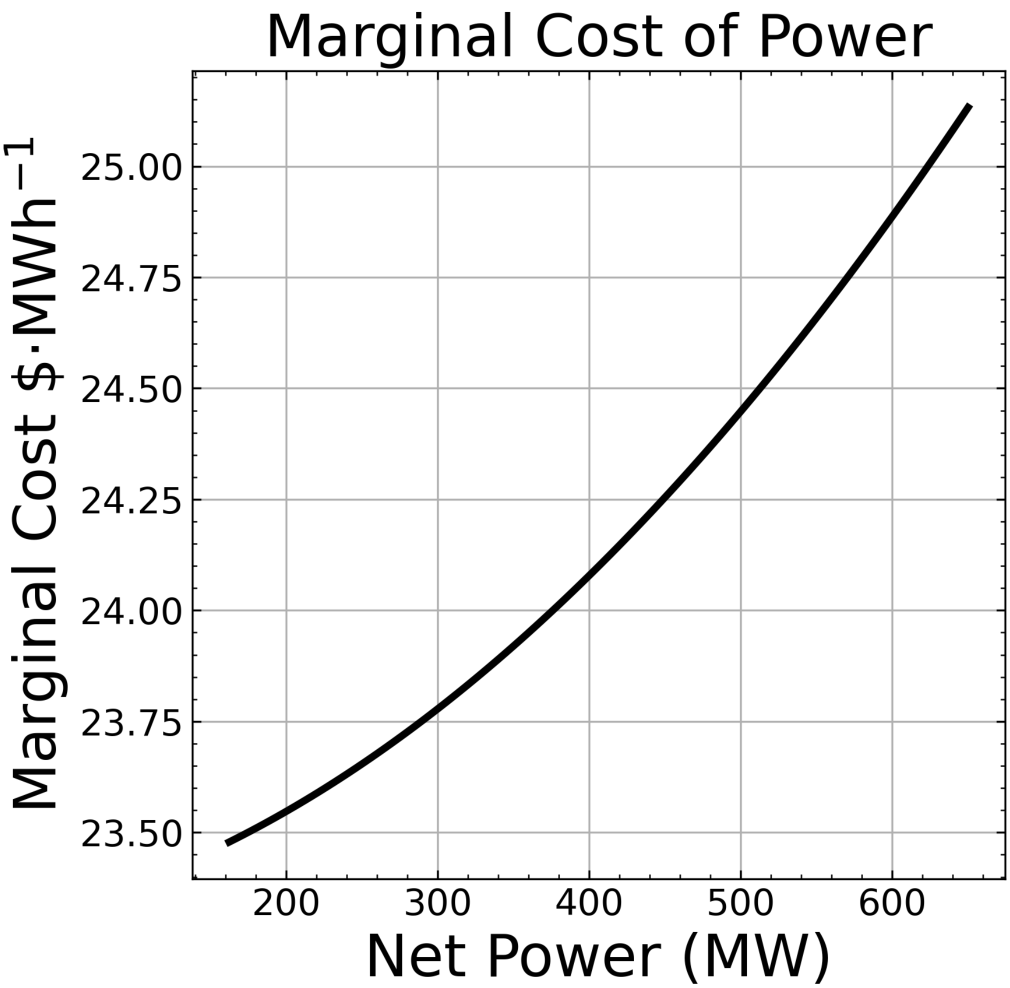

Figure S3: Marginal cost of power for standalone SOFC and rSOC in power only mode.

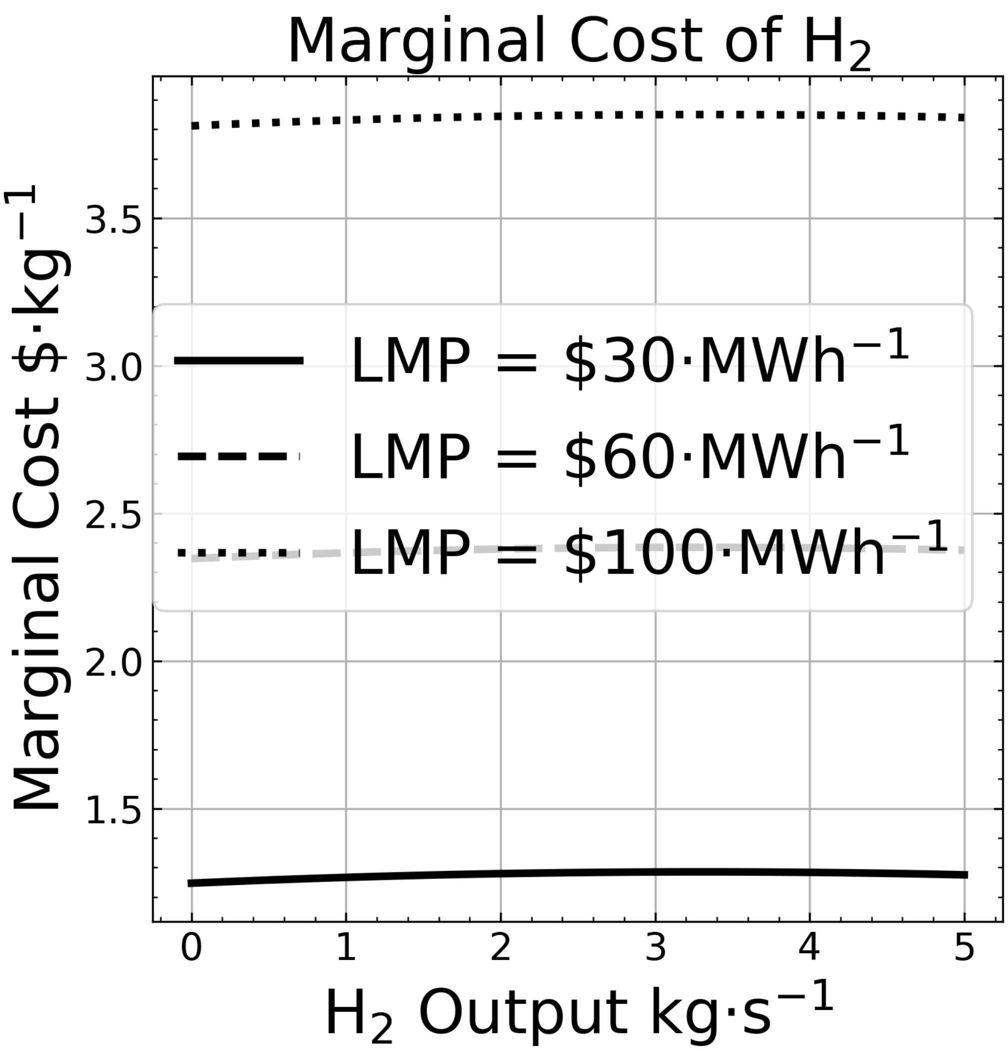

Figure S4: Marginal cost of hydrogen for standalone SOEC and rSOC in hydrogen only mode. Marginal cost plotted at three different LMP values (as electricity needs to be purchased from the grid to produce hydrogen for this process concept).

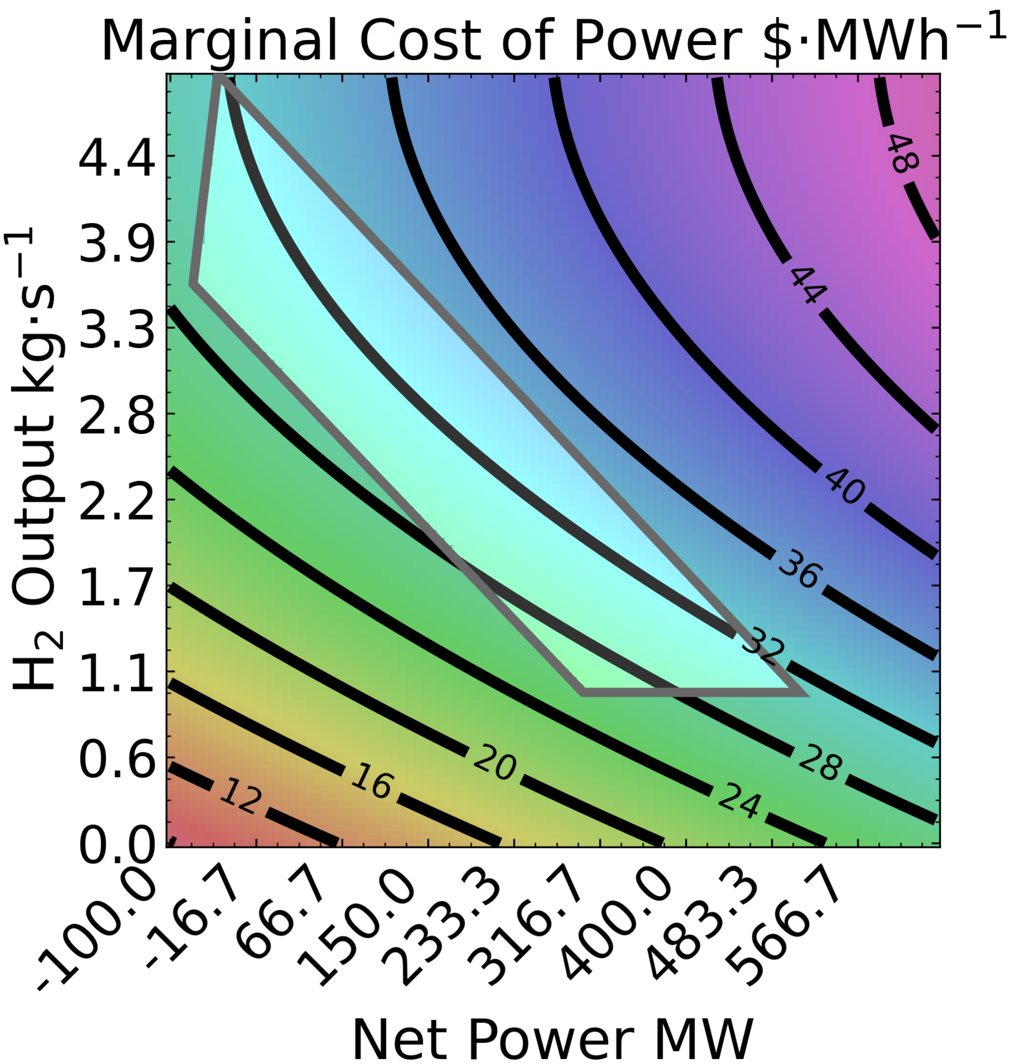

Figure S5: Marginal cost of power for the NGCC + SOEC. Contours correspond to the marginal cost values. Grey outlined box represents the feasible coproduction range - outside of this box, only one product can be produced at once (hydrogen or electricity).

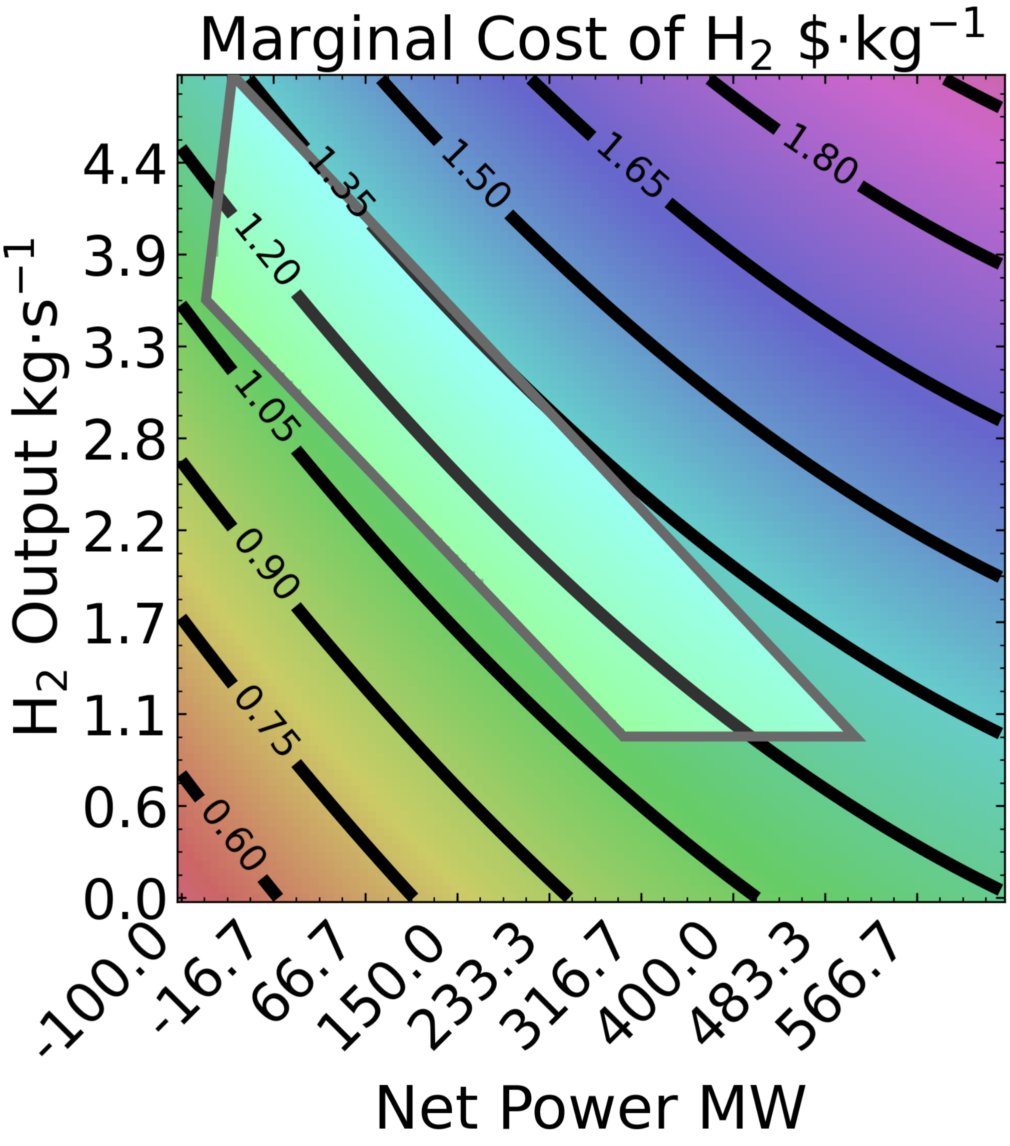

Figure S6: Marginal cost of hydrogen for the NGCC + SOEC. Contours correspond to the marginal cost values. Grey outlined box represents the feasible coproduction range - outside of this box, only one product can be produced at once (hydrogen or electricity).

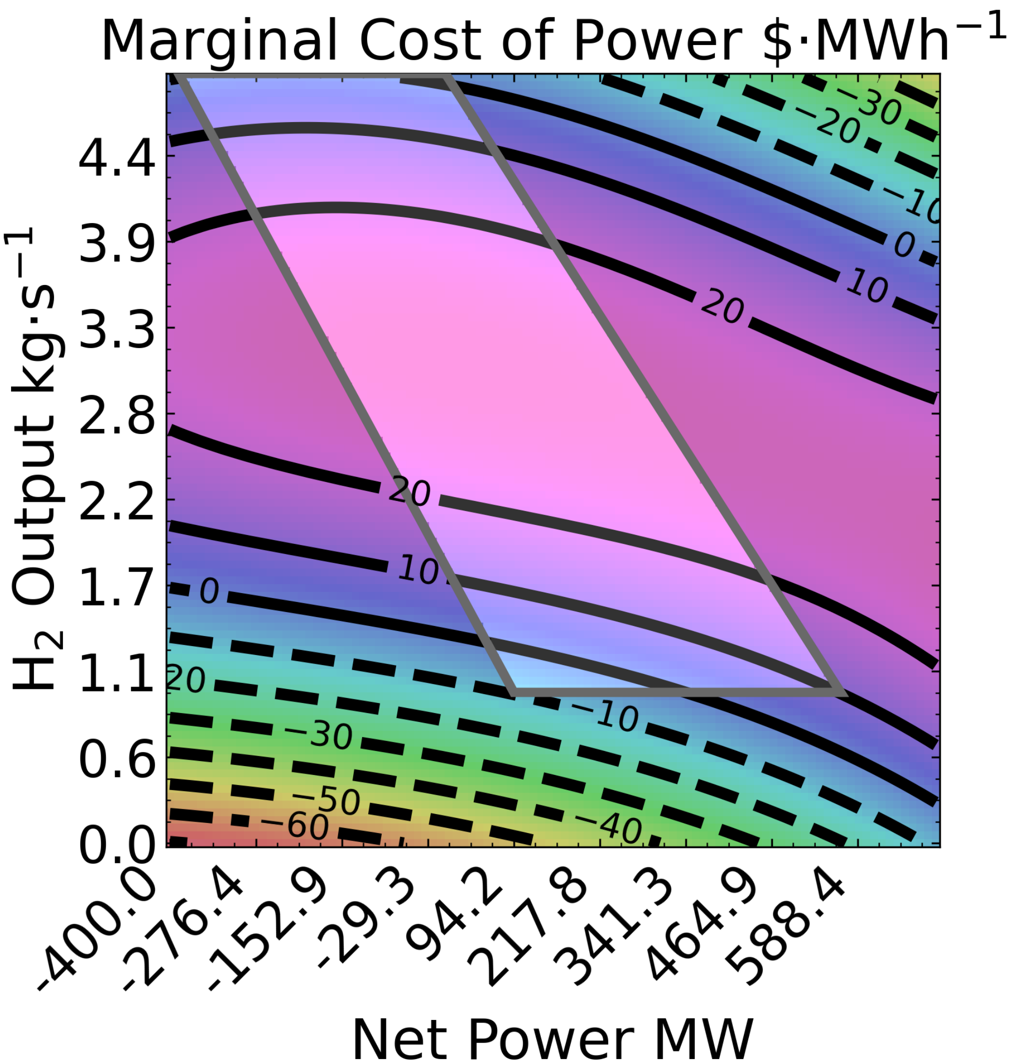

Figure S7: Marginal cost of power for the SOFC + SOEC. Contours correspond to the marginal cost values. Grey outlined box represents the feasible coproduction range - outside of this box, only one product can be produced at once (hydrogen or electricity).

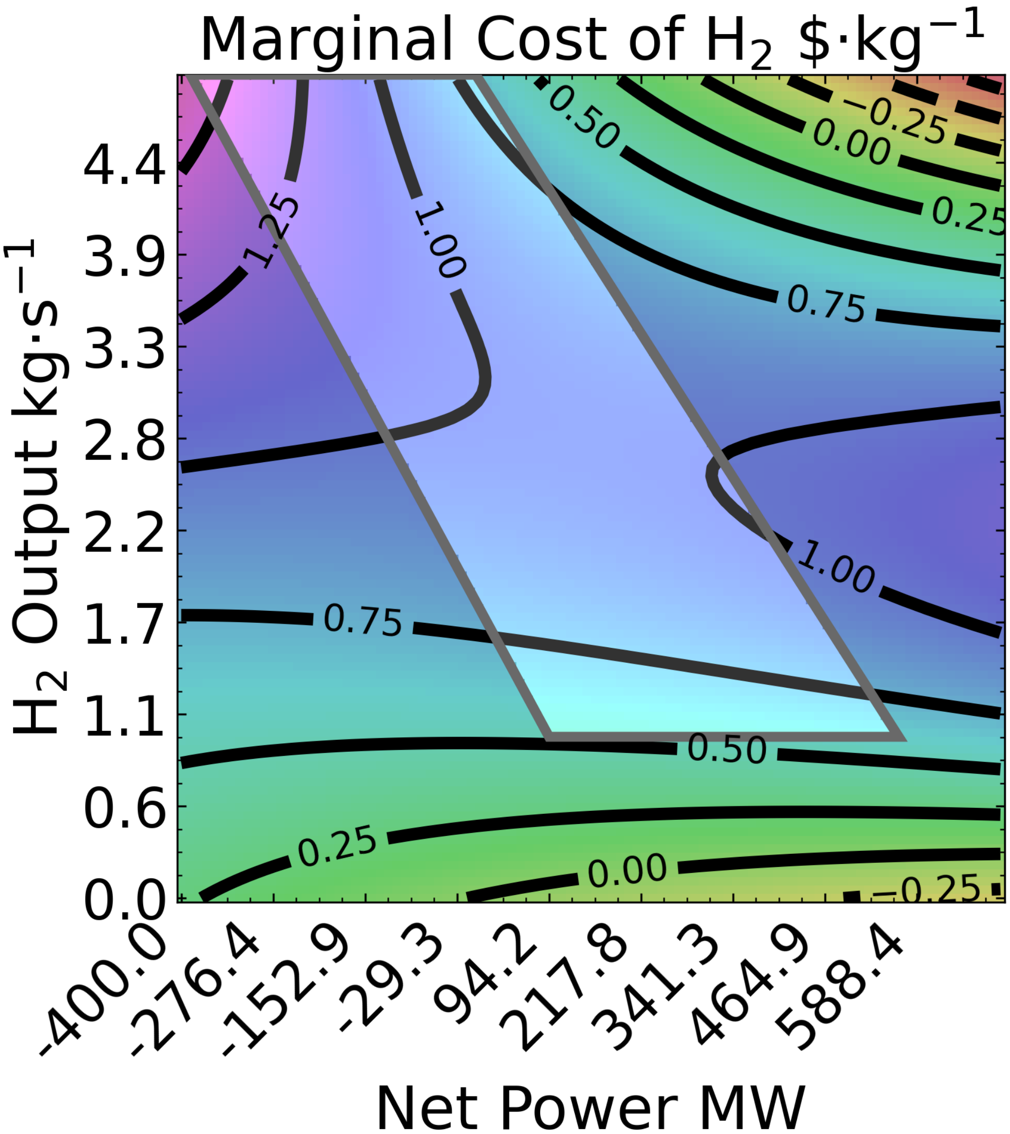

Figure S8: Marginal cost of hydrogen for the SOFC + SOEC. Contours correspond to the marginal cost values. Grey outlined box represents the feasible coproduction range - outside of this box, only one product can be produced at once (hydrogen or electricity).

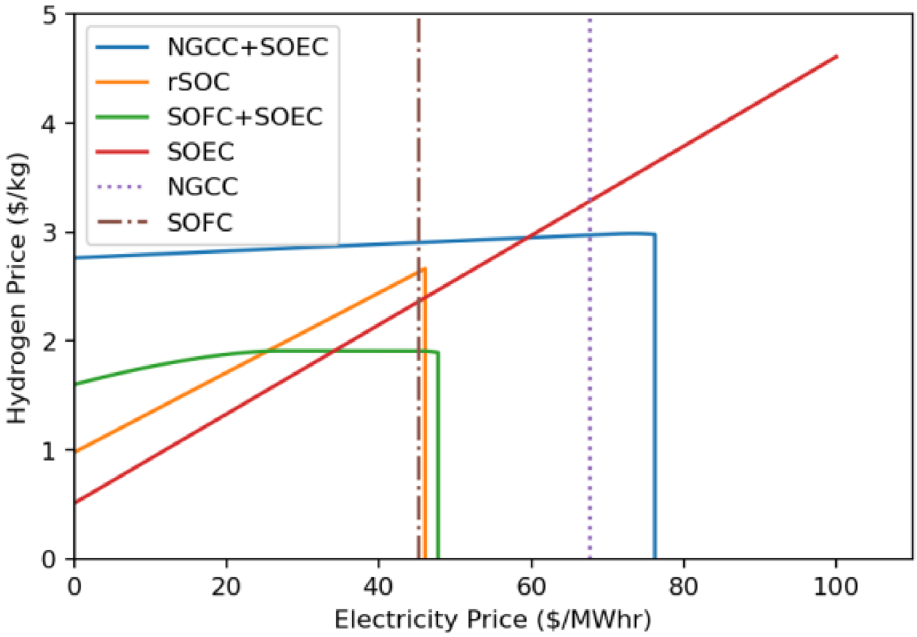

Figure S9: Break-even curves for system concepts based on electricity prices in $\$\cdot\mathrm{MWh}^{-1}$ and hydrogen prices in $\$\cdot\mathrm{kg}^{-1}$. Natural gas price $\$4.42\cdot\mathrm{MMBtu}^{-1}$. Prices in 2018 dollars [49].

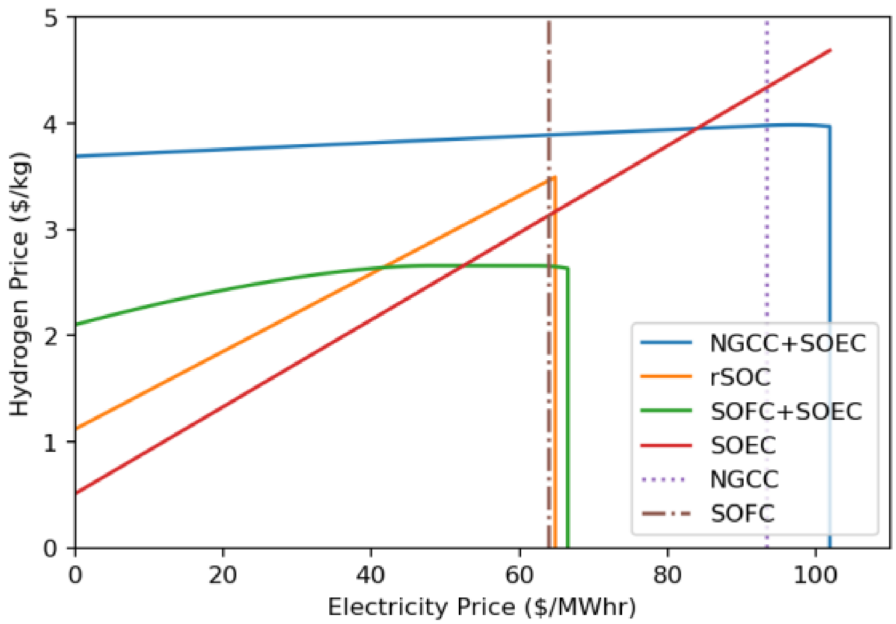

Figure S10: Break-even curves for system concepts based on electricity prices in $\$\cdot\mathrm{MWh}^{-1}$ and hydrogen prices in $\$\cdot\mathrm{kg}^{-1}$. Natural gas price $\$8\cdot\mathrm{MMBtu}^{-1}$. Prices in 2018 dollars [49].

Table S6: R^2 Values for Surrogate Equations. No R^2 value for fixed cost surrogates because they are developed from system costs, not simulation.

System	Value	R^2
NGCC	Fixed Cost ($\frac{M\$}{yr}$)	-
	Fuel Cost ($\frac{\$}{hr}$)	1.0
	Variable Cost ($\frac{\$}{hr}$)	1.0
SOFC	Fixed Cost ($\frac{M\$}{yr}$)	-
	Fuel Cost ($\frac{\$}{hr}$)	1.0
	Variable Cost ($\frac{\$}{hr}$)	1.0
NGCC + SOEC	Fixed Cost ($\frac{M\$}{yr}$)	-
	Fuel Cost ($\frac{\$}{hr}$)	0.997
	Variable Cost ($\frac{\$}{hr}$)	0.997
	Feasible Operating Range	0.992
		0.998
		0.999
		-
rSOC	Fixed Cost ($\frac{M\$}{yr}$)	-
	Fuel Cost ($\frac{\$}{hr}$) (*power only*)	1.0
	Variable Cost ($\frac{\$}{hr}$) (*power only*)	1.0
	Fuel Cost ($\frac{\$}{hr}$) (*hydrogen only*)	0.978
	Variable Cost ($\frac{\$}{hr}$) (*hydrogen only*)	1.0
	Electricity Cost ($\frac{\$}{hr}$) (*hydrogen only*)	1.0
SOFC + SOEC	Fixed Cost ($\frac{M\$}{yr}$)	-
	Fuel Cost ($\frac{\$}{hr}$) (*power + hydrogen*)	0.997
	Variable Cost ($\frac{\$}{hr}$) (*power + hydrogen*)	0.988
	Fuel Cost ($\frac{\$}{hr}$) (*power only*)	1.0

Table S6:

System	**Value**	**R^2**
SOFC + SOEC	Variable Cost ($\frac{\$}{hr}$) (*power only*)	1.0
	Feasible Operating Range	0.999
		0.998
		-
SOEC	Fixed Cost ($\frac{M\$}{yr}$)	-
	Electricity Cost ($\frac{\$}{hr}$)	1.0
	Variable Cost ($\frac{\$}{hr}$)	0.995

S8. Supplemental Optimization Results

In the main text, only an H_2 price of \$2.00$\cdot$kg^{-1} is examined in Figure 4. Therefore, all other H_2 prices (1.00, 1.50, 2.50, and 3.00 \$$\cdot$kg^{-1}) are shown in this section. Also, a market summary with markets sorted in the same fashion as these plots is shown. In this way, Figure S23 can be used to directly compare what market statistics lead to a given optimal solution. Market data are also summarized in Table S7.

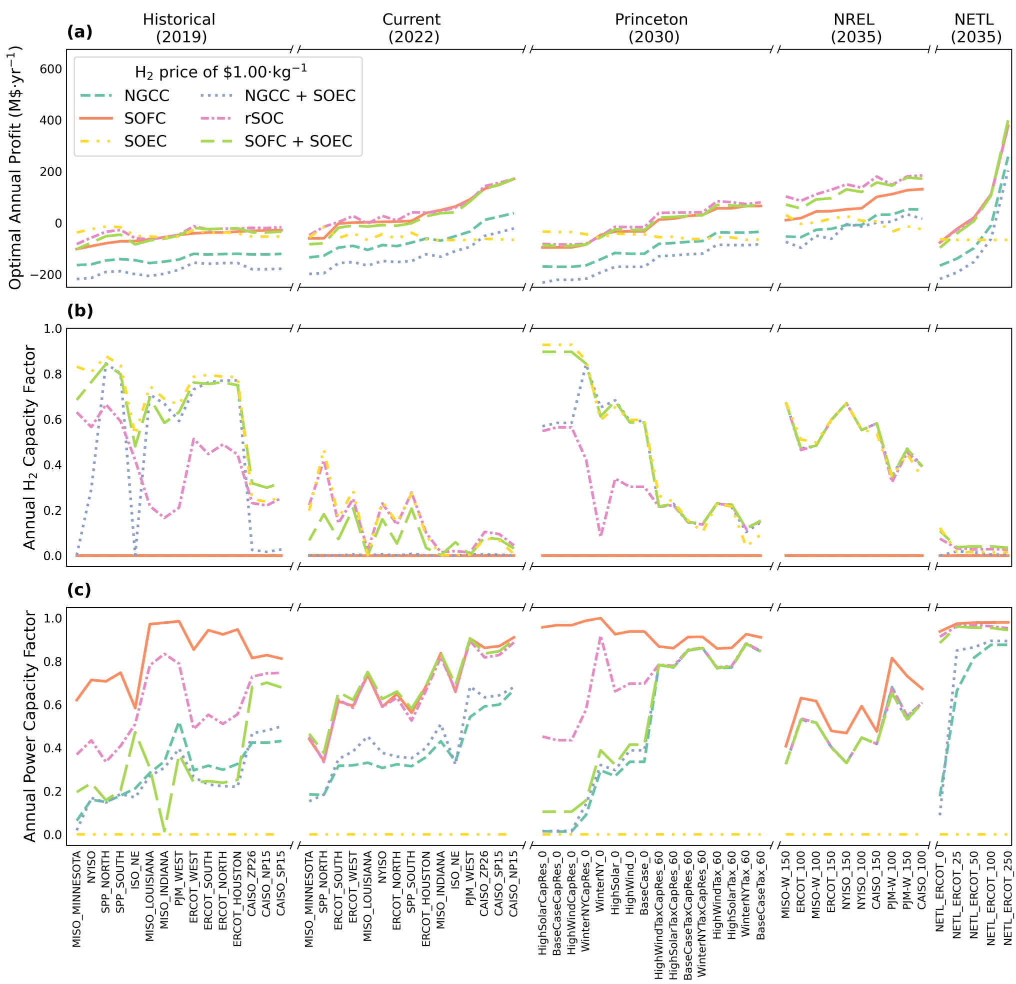

Figure S11: Optimal results for (a) Annualized profit, (b) Annual H_2 Capacity Factor, and (c) Annual Power Capacity Factor. Each market and technology are shown for an H2 price of $\$1.00 \cdot kg^{-1}$. Within each reference, markets are sorted by ascending profit for the SOFC process concept.

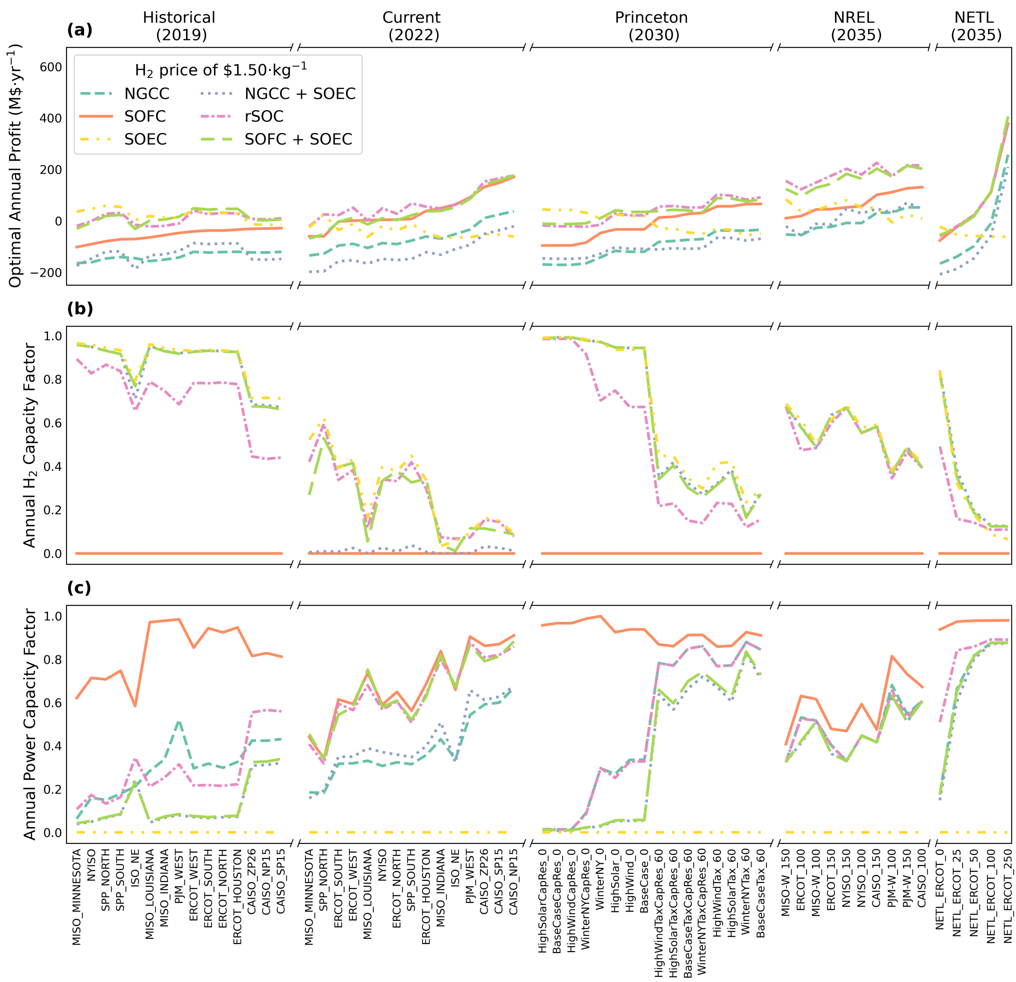

Figure S12: Optimal results for (a) Annualized profit, (b) Annual H_2 Capacity Factor, and (c) Annual Power Capacity Factor. Each market and technology are shown for an H2 price of \$1.50·kg^{-1}. Within each reference, markets are sorted by ascending profit for the SOFC process concept.

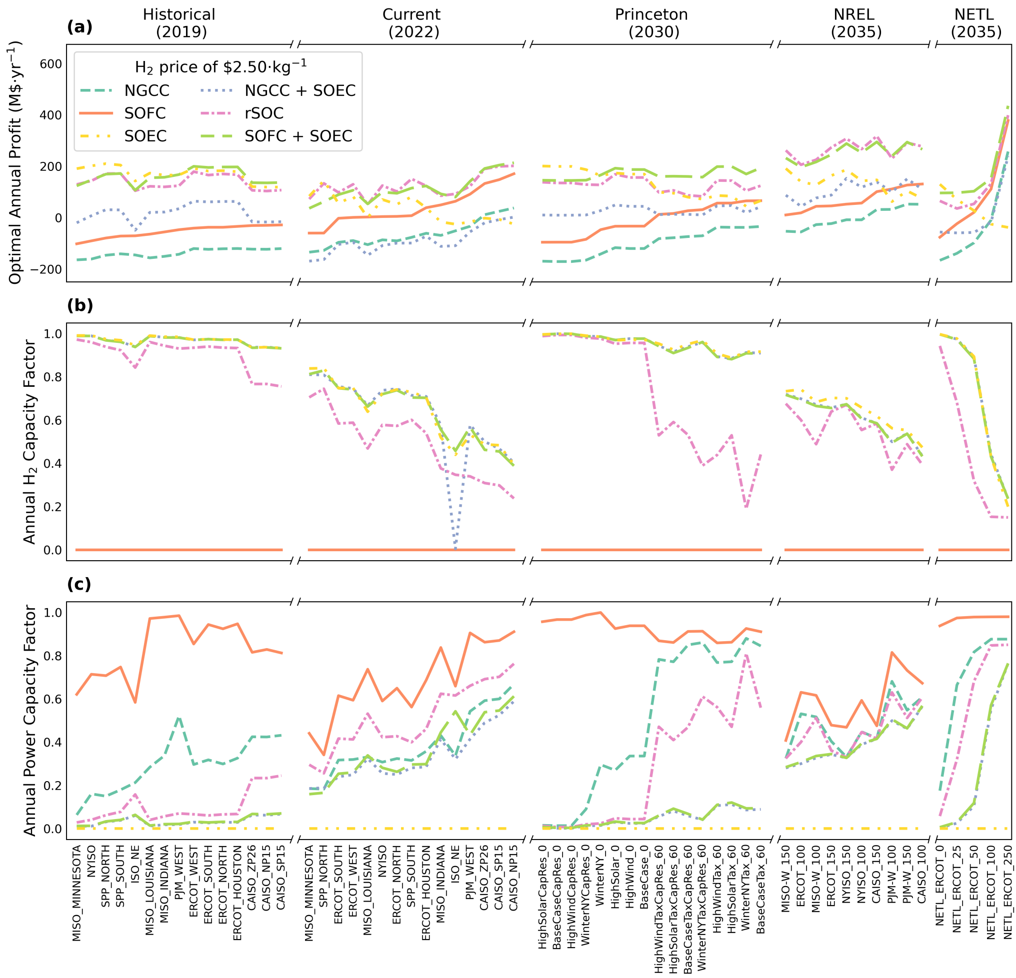

Figure S13: Optimal results for (a) Annualized profit, (b) Annual H_2 Capacity Factor, and (c) Annual Power Capacity Factor. Each market and technology are shown for an H2 price of \$2.50·kg^{-1}. Within each reference, markets are sorted by ascending profit for the SOFC process concept.

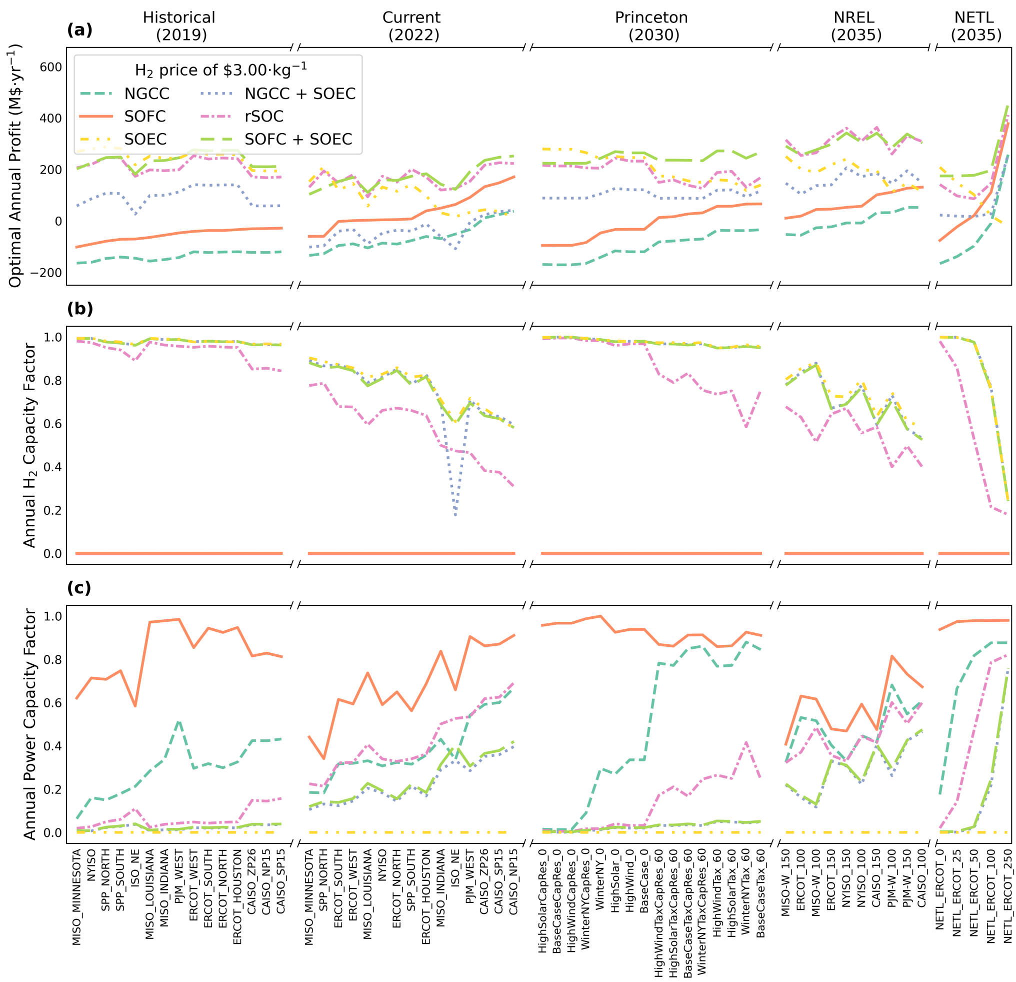

Figure S14: Optimal results for (a) Annualized profit, (b) Annual H_2 Capacity Factor, and (c) Annual Power Capacity Factor. Each market and technology are shown for an H2 price of \$3.00·kg^{-1}. Within each reference, markets are sorted by ascending profit for the SOFC process concept.

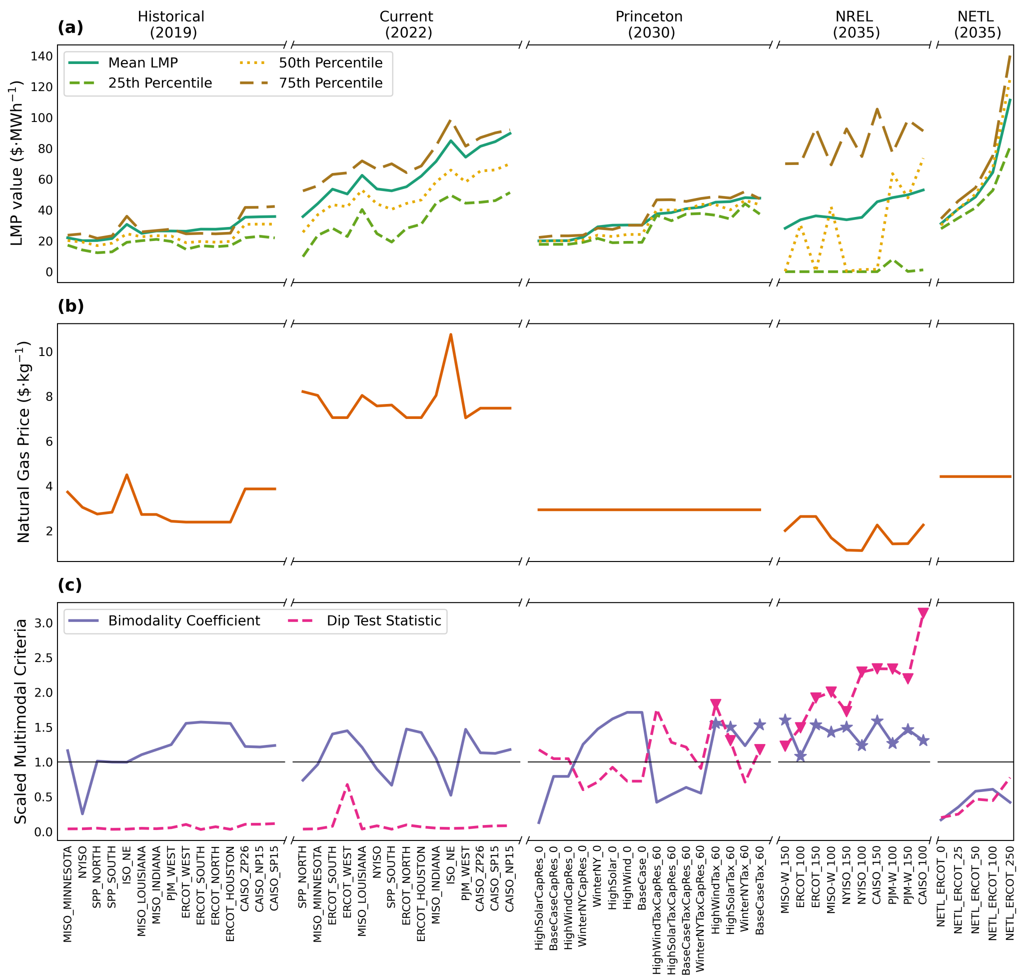

Figure S15: Summary statistics of the LMP market signals for (a) LMP Distribution Quartiles and Mean, (b) Natural Gas Price, and (c) Multimodality Test Statistics. For market signal modality, only those that have both statistics above the normalized threshold are considered to be multimodal (indicated with markers). Markets are broken down by reference. To compare with the above optimal operating solution plots, the SI version of this figure has been sorted by ascending SOFC as to align the x-axes of Figures S11 through S14.

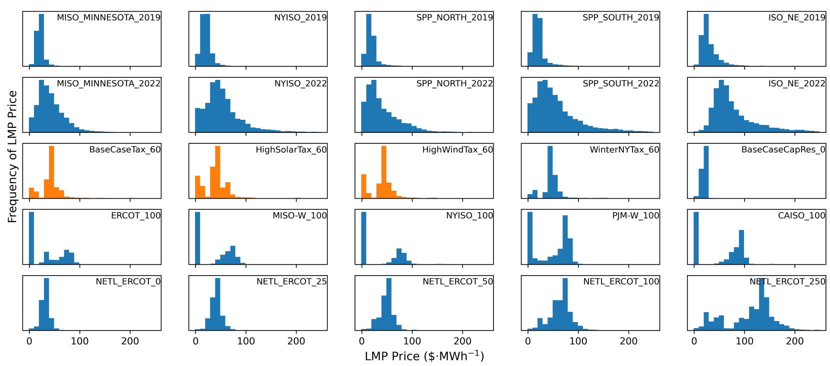

Figure S16: Sample histograms for each reference described in Section 3.4. Five markets from each reference are shown with multimodal markets in orange and unimodal markets in blue.

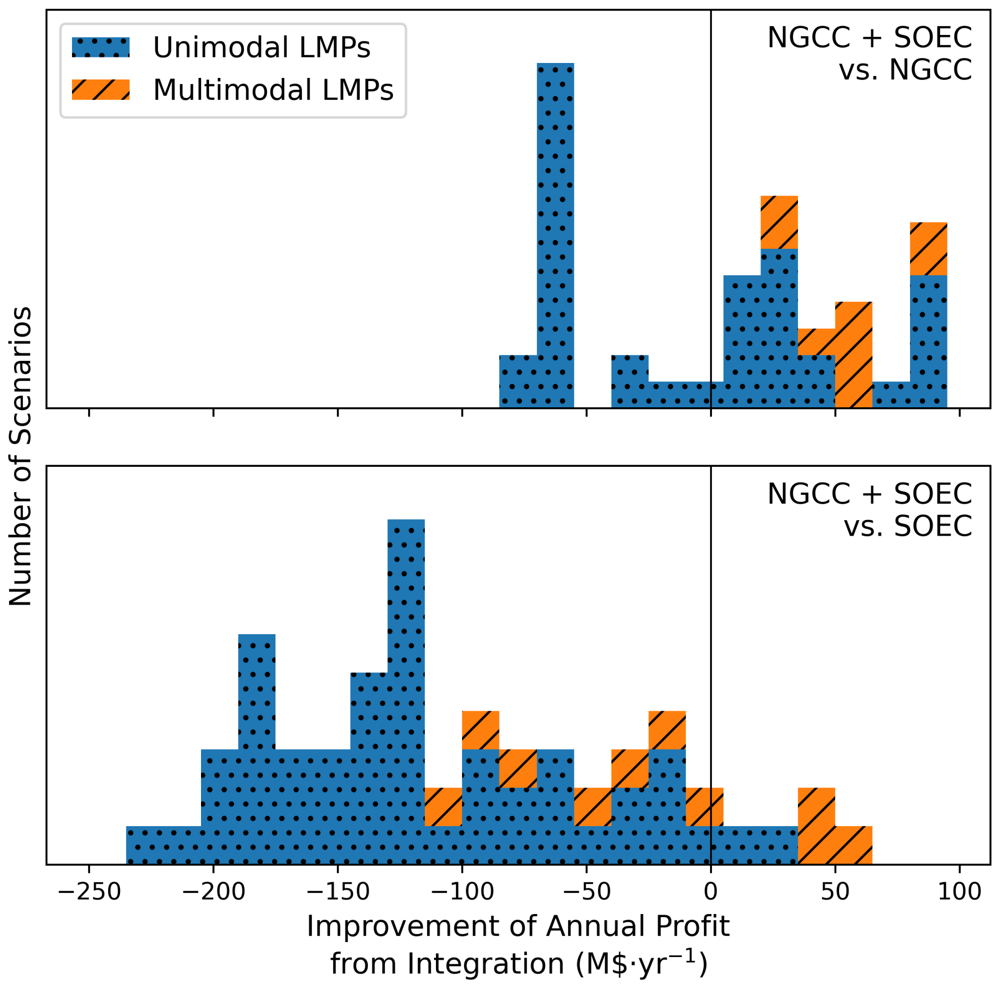

Figure S17: Here, the difference in optimized annual profits for standalone NGCC (top) and SOEC (bottom) process concepts when compared with the NGCC + SOEC integrated process concept is shown at a H_2 price of 2.00 $\$\cdot kg^{-1}$. The height of the bars indicates how many scenarios achieve a profit improvement through integration. Break even line is shown for reference (solid black). Multimodal scenarios are labeled differently to demonstrate that multimodal scenarios see large profit differences.

Table S7: Summary of Electricity Market Data

Source	LMP Signal Name	Natural Gas Price ($/MMBTU)	Carbon Tax ($/tonne)	Price Statistics ($/MWh)				
				Minimum	Maximum	Mean	Median	Standard Deviation
	CAISO_NP15_2019	3.87	0	-43.37	1013.67	35.59	30.84	37.85
	CAISO_NP15_2022	7.47	0	-16.39	1971.89	72.48	65.46	94.99
	CAISO_ZP26_2019	3.87	0	-40.62	1065.91	35.32	30.68	38.85
	CAISO_ZP26_2022	7.47	0	-35.09	1976.53	64.98	61.25	89.87
	CAISO_SP15_2019	3.87	0	-36.5	980.31	35.76	30.81	39.35
	CAISO_SP15_2022	7.47	0	-27.47	1994.73	68.58	61.89	93.21
	ERCOT_NORTH_2019	2.39	0	-10.42	4696.89	27.53	19.12	106.9
	ERCOT_NORTH_2022	7.05	0	-464.73	5073.44	56.4	46.14	130.09
	ERCOT_SOUTH_2019	2.39	0	-50.29	4694.81	27.57	19.59	105.75
	ERCOT_SOUTH_2022	7.05	0	-31.18	4680.66	54.81	45.1	114.42
	ERCOT_WEST_2019	2.39	0	-24.64	4697.2	26.2	18.79	107.59
[54]	ERCOT_WEST_2022	7.05	0	-47.61	5143.3	51.22	43.88	131
	ERCOT_HOUSTON_2019	2.39	0	-71.97	4694.64	28.2	19.63	107.06
	ERCOT_HOUSTON_2022	7.05	0	-28.79	4835.43	64.26	48.5	149.29
	ISO_NE_2019	4.5	0	-56.16	261.35	30.68	24.55	20.56
	ISO_NE_2022	10.76	0	-150.91	764.88	81.93	65.42	54.37
	NYISO_2019	3.05	0	-186.74	356.71	20.09	19.18	14.84
	NYISO_2022	7.57	0	-410.7	1215.43	53.84	46.06	54.03
	MISO_INDIANA_2019	2.73	0	2.26	936.4	26.41	23.33	21.66
	MISO_INDIANA_2022	8.04	0	-4.43	1082.57	70.07	59.29	47.31
	MISO_LOUISIANA_2019	2.73	0	-31.26	968.31	24.86	22.67	18.64
	MISO_LOUISIANA_2022	8.04	0	-3.03	1102.38	62.18	53.81	39.3
	MISO_MINNESOTA_2019	3.73	0	-38.56	661.22	21.97	20.19	16.96
	MISO_MINNESOTA_2022	8.04	0	-62.28	1111.41	44.66	37.55	39.59
	PJM_WEST_2019	2.43	0	-53	746.59	26.38	23.12	22.95
	PJM_WEST_2022	7.04	0	-20.3	2859.11	70.66	58.76	59.2
[54]	SPP_NORTH_2019	2.75	0	-46.48	1130.72	20.19	16.91	31.47
	SPP_NORTH_2022	8.21	0	-102.8	821.62	36.04	25.51	49.43
	SPP_SOUTH_2019	2.83	0	-43.72	1210.58	21.48	18.47	35.32
	SPP_SOUTH_2022	7.61	0	-38.08	871.8	52.79	40.06	60.65
	MiNg_$100_CAISO_2035	2.26	100	0	178.28	52.97	73.59	43.72
	MiNg_$150_CAISO_2035	2.26	150	0	203.01	45.35	1.53	53.74
	MiNg_$100_ERCOT_2035	2.64	100	0	186.42	33.66	30.39	35.3
	MiNg_$150_ERCOT_2035	2.64	150	0	204.49	36.18	0.18	46.6
[56]	MiNg_$100_MISO-W_2035	1.69	100	0	145.07	35.12	42.12	34.45

Source	LMP Signal Name	Natural Gas Price ($/MMBTU)	Carbon Tax ($/tonne)	Price Statistics ($/MWh)				
				Minimum	Maximum	Mean	Median	Standard Deviation
	MiNg_$150_MISO-W_2035	2.01	150	0	162.06	28.13	0.25	40.39
	MiNg_$100_NYISO_2035	1.12	100	0	182.14	35.22	1.41	40.06
	MiNg_$150_NYISO_2035	1.14	150	0	229.17	33.67	0.27	48.61
	MiNg_$100_PJM-W_2035	1.42	100	0	172.29	48.01	63.58	33.48
	MiNg_$150_PJM-W_2035	1.43	150	0	181.06	49.81	47.84	45.76
[59]	BaseCase_2030	2.94	0	-113.28	1349.59	30.25	24.13	80.53
	HighWind_2030	2.94	0	-113.28	1349.59	30.25	24.13	80.53
	HighSolar_2030	2.94	0	-111.29	1800	30.13	22.77	91.84
	WinterNY_2030	2.94	0	0	4257.43	29.09	23.73	81.73
	BaseCaseTax_2030	2.94	60	0	1800	47.69	43.4	82.48
	HighWindTax_2030	2.94	60	0	1800	45.06	43.4	89.51
	HighSolarTax_2030	2.94	60	0	1800	45.43	40.1	85.88
	WinterNYTax_2030	2.94	60	0	1800	48	46.22	44.47
	BaseCaseCapRes_2030	2.94	0	-330.01	111.65	20.11	19.98	8.71
	HighWindCapRes_2030	2.94	0	-330.01	111.65	20.11	19.98	8.71
	HighSolarCapRes_2030	2.94	0	-266.22	123.82	19.96	19.62	8.82
	WinterNYCapRes_2030	2.94	0	0	135.51	22.36	20.52	9.7
	BaseCaseTaxCapRes_2030	2.94	60	0	209.1	40.85	40.1	23.25
	HighWindTaxCapRes_2030	2.94	60	0	202.88	37.49	40.1	23.91
	HighSolarTaxCapRes_2030	2.94	60	-1.95	205.3	38.28	39.91	25.24
	WinterNYTaxCapRes_2030	2.94	60	0	223.23	41.83	43.68	21.03
[76]	NETL_ERCOT_GEN_0	4.42	0	0.13	193.14	31.14	30.14	8.66
	NETL_ERCOT_GEN_25	4.42	27.56	0.13	345.55	40.7	40.67	11.92
	NETL_ERCOT_GEN_50	4.42	55.12	0.13	841.25	48.45	50.32	17.65
	NETL_ERCOT_GEN_100	4.42	110.23	0.13	1167.41	64.34	67.53	27.2
	NETL_ERCOT_GEN_250	4.42	275.58	0.13	1289.15	111.26	125.27	56.15

S9. Process Alternatives Detailed Figures

The following section includes all integrated energy system alternatives as full size figures.

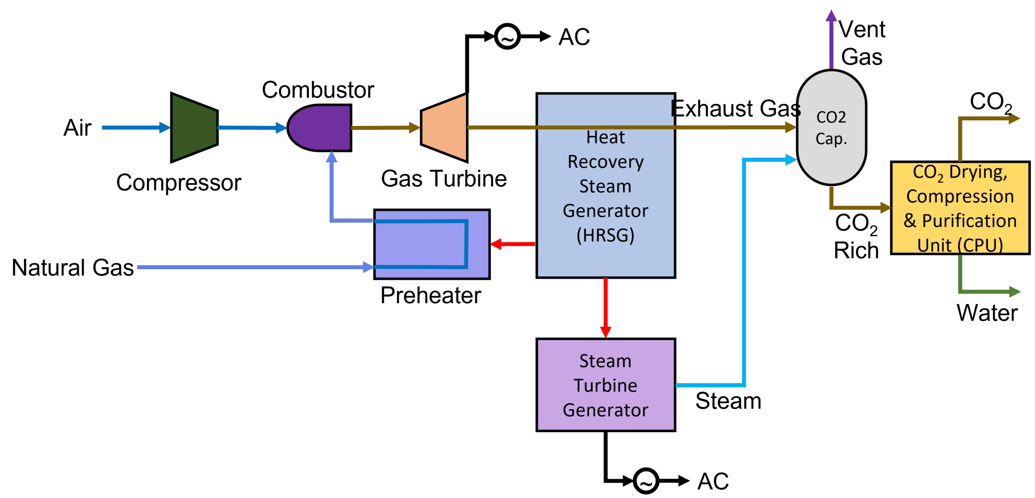

Figure S18: Full size schematic of the NGCC process.

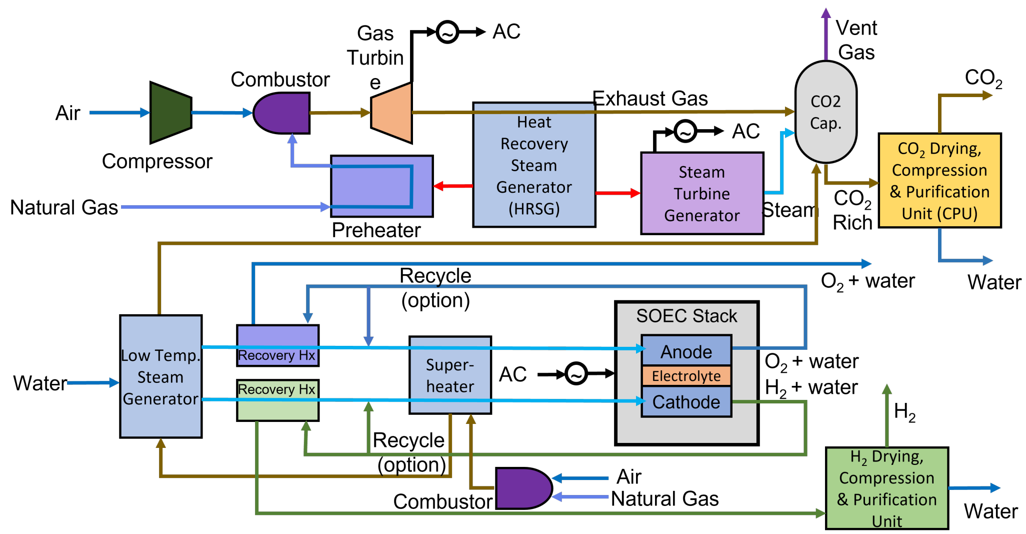

Figure S19: Full size schematic of the NGCC + SOEC process.

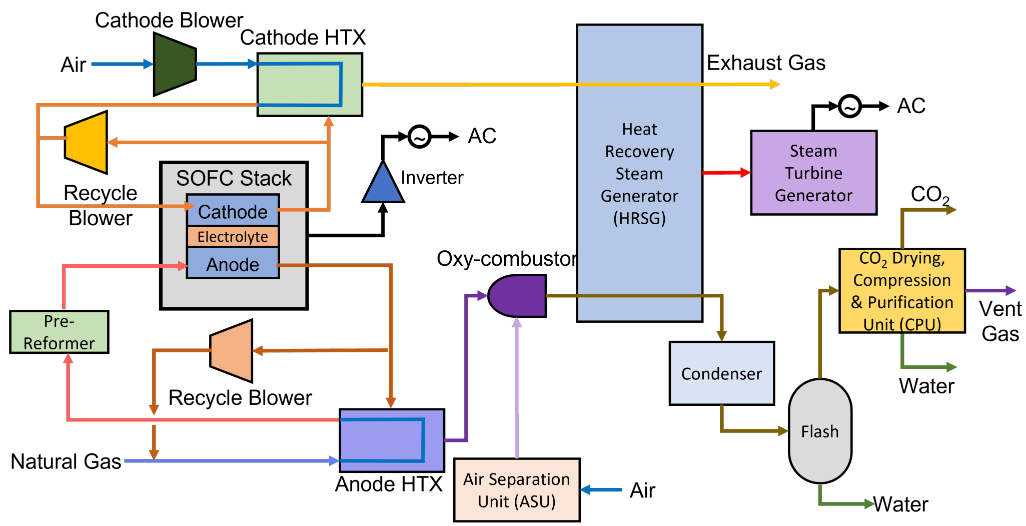

Figure S20: Full size schematic of the SOFC process.

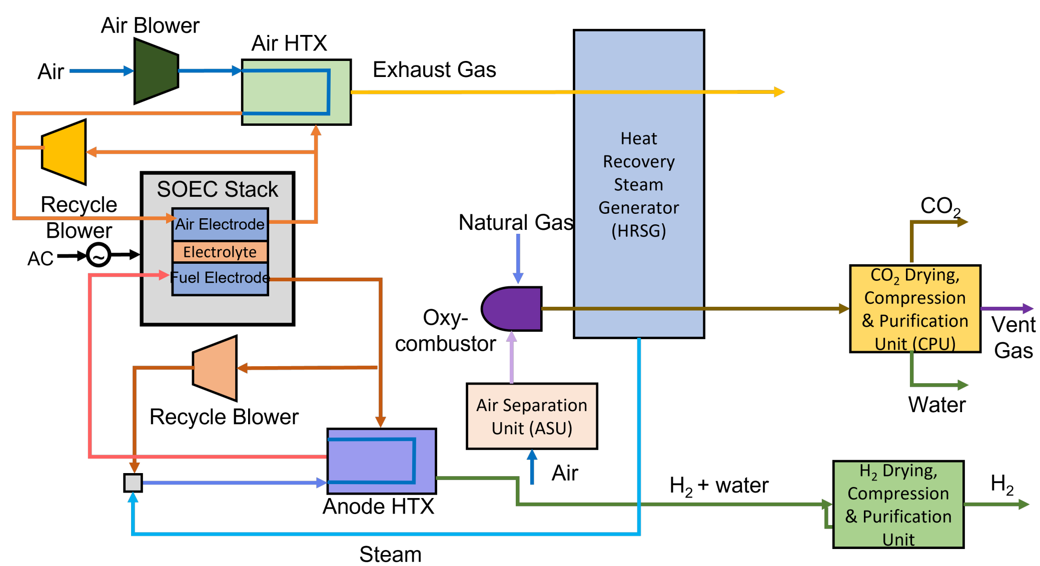

Figure S21: Full size schematic of the SOEC process.

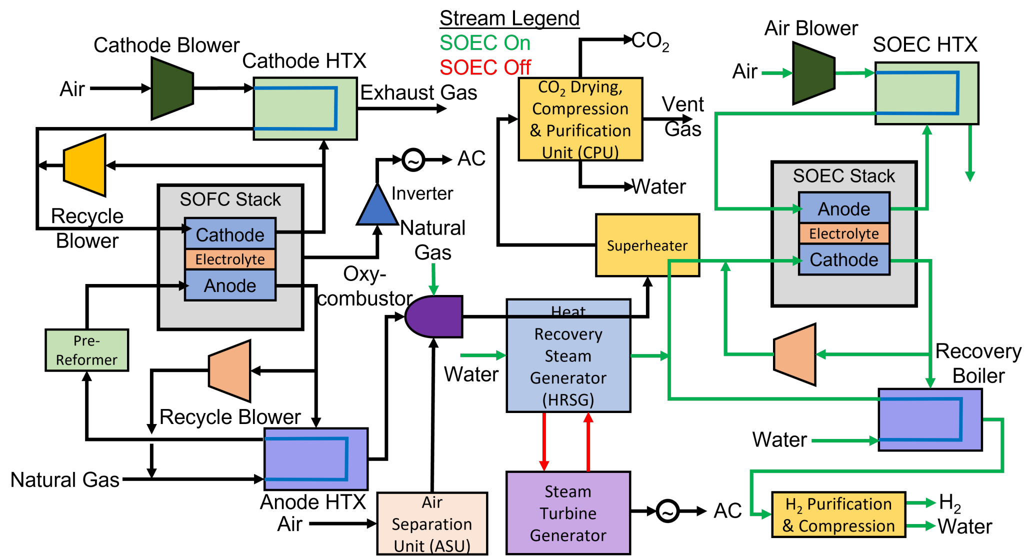

Figure S22: Full size schematic of the SOFC + SOEC process.

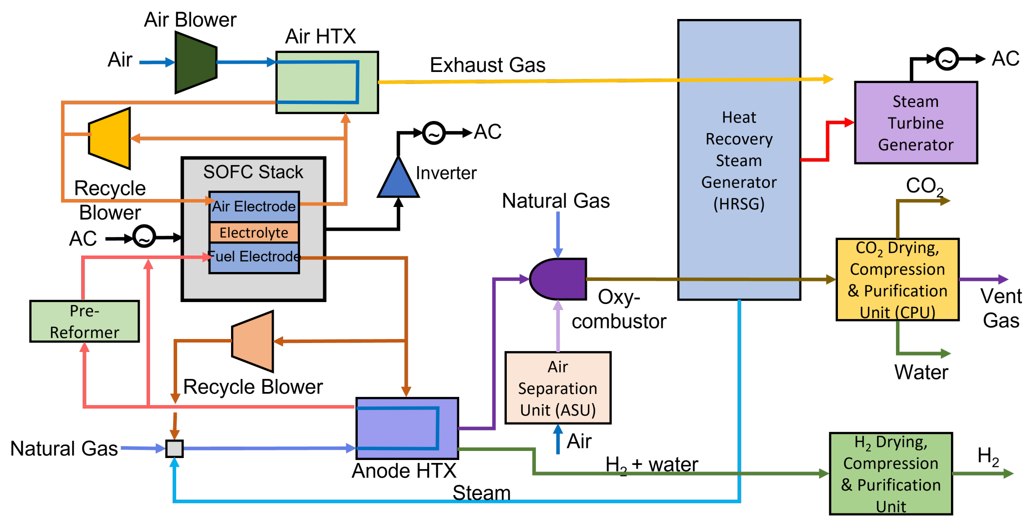

Figure S23: Full size schematic of the rSOC process.